THE JOURNAL OF BIOLOGICAL CHEMISTRY
Vol. 275, No. 13, Issue of March 31, pp. 9340–9347, 2000

Printed in U.S.A.

TASK-3, a New Member of the Tandem Pore K^+ Channel Family*

(Received for publication, October 21, 1999, and in revised form, January 12, 2000)

Yangmi Kim, Hyoweon Bang‡, and Donghee Kim§

From the Department of Physiology and Biophysics, Finch University of Health Sciences/The Chicago Medical School, North Chicago, Illinois 60064

We have isolated from the rat cerebellum cDNA library a complementary DNA encoding a new member of the tandem pore K^+ channel family. Its amino acid sequence shares 54% identity with that of TASK-1, but less than 30% with those of TASK-2 and other tandem pore K^+ channels (TWIK, TREK, TRAAK). Therefore, the new clone was named TASK-3. Reverse transcriptase-polymerase chain reaction analysis showed that TASK-3 mRNA is expressed in many rat tissues including brain, kidney, liver, lung, colon, stomach, spleen, testis, and skeletal muscle, and at very low levels in the heart and small intestine. When expressed in COS-7 cells, TASK-3 exhibited a time-independent, noninactivating K^+-selective current. Single-channel conductance was 27 pS at −60 mV and 17 pS at 60 mV in symmetrical 140 mM KCl. TASK-3 current was highly sensitive to changes in extracellular pH (pH_o), a hallmark of the TASK family of K^+ channels. Thus, a change in pH_o from 7.2 to 6.4 and 6.0 decreased TASK-3 current by 74 and 96%, respectively. Mutation of histidine at position 98 to aspartate abolished pH_o sensitivity. TASK-3 was blocked by barium (57%, 3 mM), quinidine (37%, 100 μM), and lidocaine (62%, 1 mM). Thus, TASK-3 is a new member of the acid-sensing K^+ channel subfamily (TASK).

Potassium (K^+) channels are involved in a variety of cellular functions including regulation of neuronal firing rate, heart rate, muscle contraction, and hormone secretion. Mammalian K^+ channels can now be grouped into three main structural classes with each subunit possessing two, four, or six transmembrane segments (1–3). A structurally different K^+ channel having eight transmembrane segments has been cloned from yeast (4–6), but a similar channel subunit has not been identified in the mammalian system. Despite the structural diversity, all K^+ channel subunits share a conserved P domain that is essential for providing K^+ selectivity (7–9). In *Caenorhabditis elegans*, ~50 putative K^+ channels subunits possessing two pore-forming domains and four transmembrane segments (2P/4TM)[1] have been identified by searching the genome sequences (10, 11). Recent cloning efforts have led to the identification of several members of the 2P/4TM K^+ channels. Open rectifier K^+ channel (ORK1) from *Drosophila melanogaster* and tandem of P domains in a weak inward rectifying K^+ channel (TWIK-1) from human kidney were the first two members of this family to be cloned (12, 13). Recent studies now indicate that TWIK-1 does not form a functional ion channel, whereas the open rectifier K^+ channel 1 does (14, 15). Subsequently, other members of this family were cloned using expressed sequence tags identified by searching the GenBank™ data base for TWIK-1-like sequences or using degenerate primers designed to amplify a DNA fragment with sequences homologous to TWIK-1. Electrophysiological studies of 4TM K^+ channels suggest that most behave as background K^+ currents (ORK1, TASK, TREK, TRAAK), although some have additional properties such as sensitivity to mechanical stretch, free fatty acids (TREK, TRAAK (16–19)), and extracellular pH (TASK (20, 21)). Two other 4TM K^+ channel members (KCNK6/7) were not expressed in the plasma membrane when transfected into *Xenopus* oocytes, COS-7, or HEK293 cells (22). As 2P/4TM K^+ channels generally share less than 30% amino acid identity, they are likely to be involved in diverse physiological processes.

Of the 2P/4TM K^+ channel family, two members have been named TASK-1 and TASK-2 (for TWIK-related Acid-sensitive K^+ channel), as they exhibit high sensitivity to extracellular pH near the physiological range (20, 21). Despite the overall structural conservation (2P/4TM) and similar pH sensitivity, TASK-1 and TASK-2 share only 27% amino acid identity, and the expression patterns of their mRNA transcripts in mouse tissues are different (21). According to Northern blot analysis, TASK-1 is expressed mainly in the mouse heart and lung, whereas TASK-2 is expressed primarily in the kidney, pancreas, liver, and placenta. Both TASK-1 and TASK-2 exhibit functional K^+ currents with properties of a "background" current when expressed heterologously, suggesting that one of their functions may be to help set the resting membrane potential. In rat atrial and ventricular myocytes where TASK-1 mRNA are expressed (23, 24), we were able to identify a K^+ channel with kinetic properties indistinguishable from those of TASK-1 transiently expressed in mammalian cells (24), indicating that TASK-1 encodes a functional K^+ channel that exists in mammalian cells.

In this study, we report the cloning of TASK-3 (KCNK9)[2], a new member of the TASK family, and describe its electrophysiological and pharmacological properties and tissue expression. TASK-3 shares 54% amino acid identity with TASK-1 but less than 30% with other 2P/4TM K^+ channels. Our results show that TASK-3 mRNA is expressed in many tissues but at rela-

* This work was supported by the National Institutes of Health Grant HL55363 and a grant-in-aid from the American Heart Association. The costs of publication of this article were defrayed in part by the payment of page charges. This article must therefore be hereby marked "*advertisement*" in accordance with 18 U.S.C. Section 1734 solely to indicate this fact.

The nucleotide sequence(s) reported in this paper has been submitted to the GenBank™/EBI Data Bank with accession number(s) AF192366 (TASK-3 gene).

‡ Permanent address: Dept. of Physiology, Chung-Ang University, Seoul 156–756, Korea.

§ To whom correspondence should be addressed: Dept. of Physiology & Biophysics, Chicago Medical School, 3333 Green Bay Rd., North Chicago, IL 60064. Tel.: (847)578–3280; Fax: (847)578–3265; E-mail: donghee.kim@finchcms.edu.

[1] The abbreviations used are: P, pore; TM, transmembrane; TWIK, tandem of P domains in a weak inward rectifying K^+ channel; TASK, twik-related acid-sensitive K^+ channel; bp, base pair(s); kb, kilobase; PCR, polymerase chain reaction; RT, reverse-transcriptase; GFP, green fluorescent protein; pS, picosiemens; GTPγS, guanosine 5′-3-*O*-(thio)triphosphate.

[2] TASK3 has been given the gene name KCNK9 (approved by HUGO).

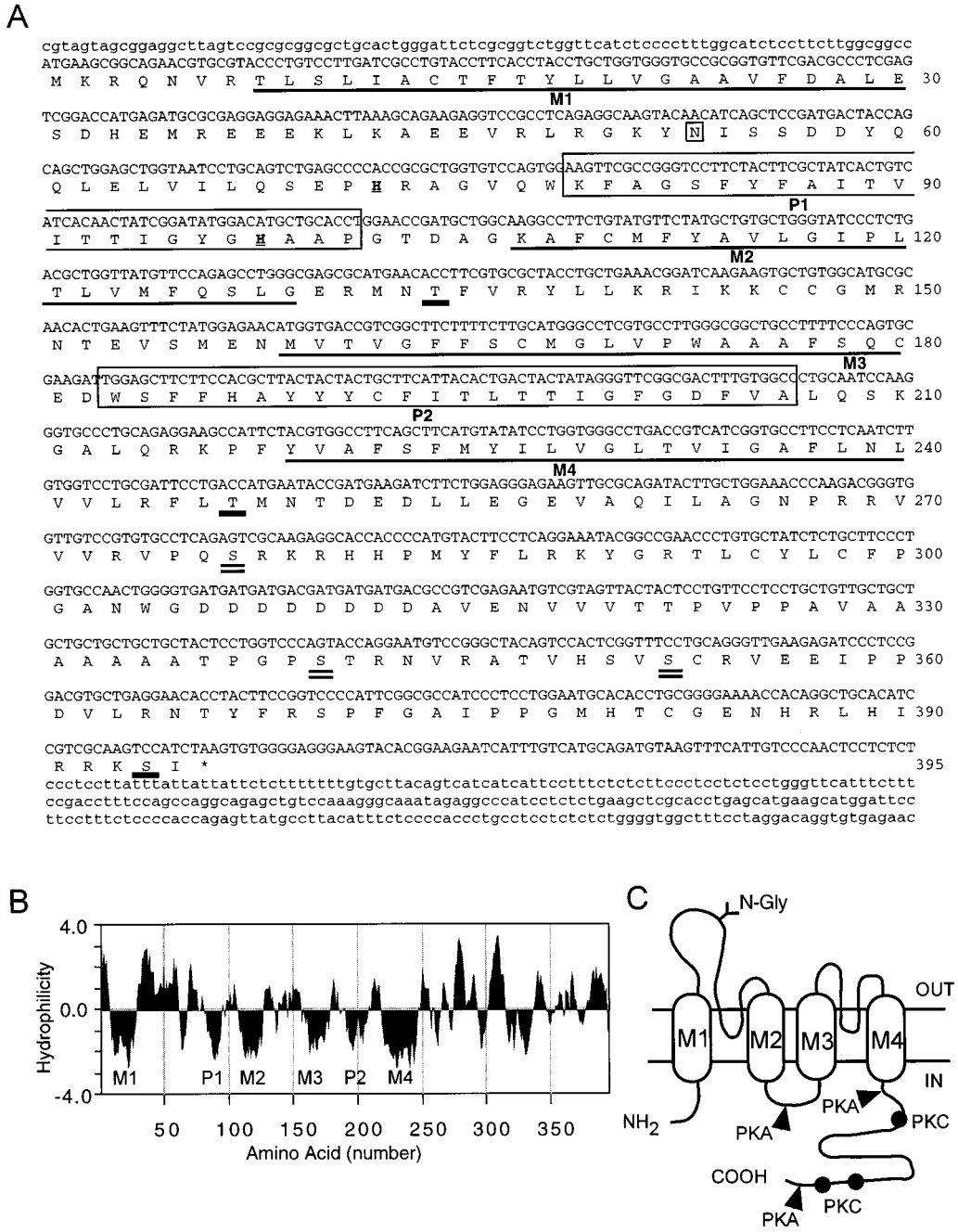

FIG. 1. *A,* nucleotide and amino acid sequences of rat TASK-3 (KCNK9). Four transmembrane segments and two P domains are *underlined* and *boxed*, respectively. Consensus sites for *N*-glycosylation (*square*), phosphorylation by protein kinase A (*thick underline*), and protein kinase C (*double underlines*) are shown. These sites were identified using the MacVector Program. *B,* hydropathy plot of TASK-3 amino acid sequence using the Kyte-Doolittle algorithm shows four potential transmembrane segments and two potential pore-forming regions. *C,* deduced topology of TASK-3. Intracellular phosphorylation sites and an extracellular *N*-glycosylation (*N-Gly*) site are shown. *PKA*, protein kinase A; *PKC,* protein kinase C.

tively very low levels in the heart, indicating that TASK-3 is unlikely to be the functional partner for TASK-1 in the rat heart. When expressed in COS-7 cells, TASK-3 exhibited an instantaneous and noninactivating K^+-selective current with high sensitivity to extracellular pH. The sensitivity to pH_o was conferred by the histidine residue at position 98 that is located near the selectivity filter of the channel pore. Thus, TASK-3 may help to set the resting membrane potential and contribute to the pH_o-dependent K^+ conductance in different types of cells.

MATERIALS AND METHODS

Cloning of TASK-3—Rat heart and cerebellum cDNA libraries (λZAPII, Stratagene) were screened with the *Hin*dIII-*Kpn*I DNA fragment (560 bp) of mouse TASK-1 using a mild stringency wash condition as described previously (23). No positive plaque was obtained from the heart cDNA library. Of 10^6 plaques screened using the cerebellum cDNA library, one positive colony was found to contain a 1.7-kb insert. DNA sequencing showed that this clone (designated 4f) contained a partial sequence of a new 4TM K^+ channel, as judged by the presence of two P domains with amino acids Gly-Tyr-Gly and Gly-Phe-Gly within these regions, respectively. A search of the GenBank™ data base indicated that the new K^+ channel clone was ~60% similar to TASK-1. To obtain the full sequence, we prepared a 496-bp DNA fragment of 4f by PCR using two specific primers (5′-TGACTACTATAGGGTTCGGC-3′ and 5′-AAGTAGGTGTTCCTCAGCACG-3′) as a probe to rescreen the rat cerebellum cDNA library. After several rounds of screening, the inserts from positive plaques were excised from the phage DNA into pBluescript SK^- vector. The inserts were analyzed by restriction en-

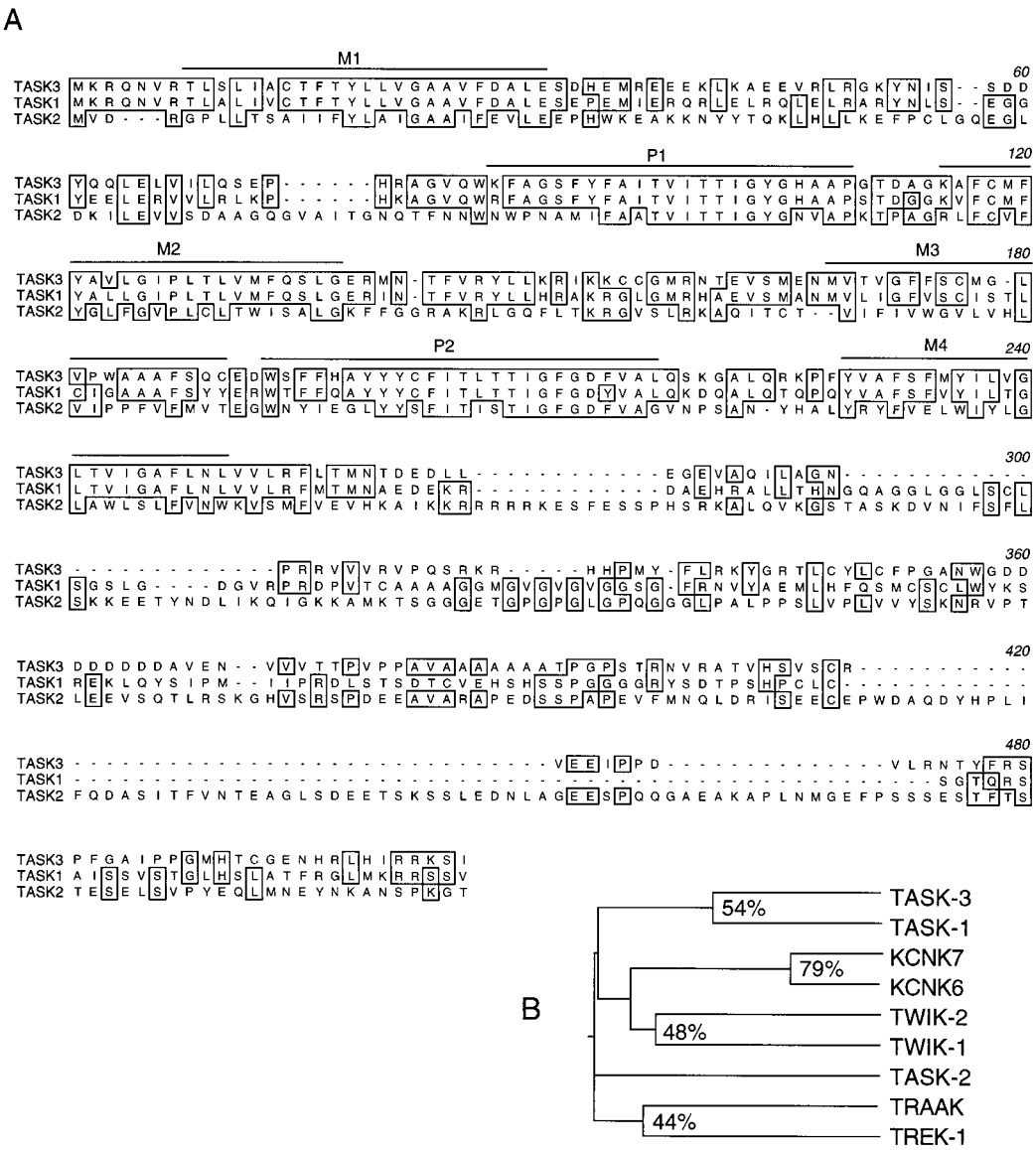

FIG. 2. **Alignment of amino acid sequences of three TASK channels: rat TASK-1 (GenBank™ accession number AF031384), human TASK-2 (GenBank™ accession number AF084830), and rat TASK-3 (GenBank™ accession number AF192366).** Identical amino acids are *outlined*. *Dashes* indicate gaps in alignment. Four TM segments and two P regions are shown. A proposed phylogenetic tree of mammalian 4TM K^+ channels is shown. The percent values indicate amino acid identity.

zymes and by sequencing of both strands using the dideoxynucleotide chain termination method. One clone contained the entire coding sequence of the new K^+ channel, which we named TASK-3. Single amino acid mutations were performed using QuikChange site-directed mutagenesis kit (Stratagene).

Tissue Distribution of TASK-3—Rat multiple tissue Northern blots were purchased from OriGene Technologies, Inc. A TASK-3-specific probe (827 bp) was prepared by PCR using a primer pair (5′-AGCTTCAGAGAGGATGGGCCTCTAT-3′ and 5′-AAGTAGGTGTTCCTCAGCACG-3′) and included the 3′-end of the coding sequence that has low homology with TASK-1. Prehybridization (4 h, 42 °C) and hybridization (overnight, 42 °C) were carried out using ^{32}P-labeled DNA probe. Blots were washed in solution containing 0.1% SDS and 2× SSC for 20 min at room temperature and then in solution containing 0.1% SDS and 0.2% SSC for an additional 10–20 min at 50 °C. Blots were exposed to x-ray film for 24–72 h before developing. For RT-PCR experiments, total RNA was isolated from 14 rat tissues (cerebrum, cerebellum, aorta, atrium, ventricle, kidney, liver, lung, colon, stomach, spleen, testis, skeletal muscle, and small intestine) using RNA STAT-60 (TEL-TEST). Total RNA (2 μg) was reverse transcribed to generate first strand cDNA with a Superscript Pre-amplification System (Life Technologies, Inc.). PCR was carried out with TASK-3-specific primers that yield the 496-bp TASK-3 fragment (see above). As control, glyceraldehyde-3-phosphate dehydrogenase was amplified using specific primers (CLONTECH). PCR conditions were 30 cycles of 45 s at 94 °C, 1 min at 55 °C, and 2 min at 72 °C. Amplified products were subcloned into pCR2.1 vector and sequenced on one strand to confirm the PCR product as TASK-3.

Transfection of TASK-3 into COS-7 Cells—For transfection into the COS-7 cell, 2.1-kb DNA containing the entire coding region was subcloned into pCDNA3.1 vector (Invitrogen) by ligating into the *Eco*RV-*Hin*dIII sites after cutting TASK-3/pBluscript SK$^-$ with *Dra*I and *Hin*dIII. COS-7 cells were seeded at low density (25,000 cells/35-mm dish) for 1 day prior to transfection. COS-7 cells were co-transfected with TASK-3 and green fluorescent protein (GFP) (CLONTECH) in pcDNA3.1 using LipoTaxi (Life Technologies, Inc.) transfection reagent. Green fluorescence from GFP-expressing cells was identified using a Nikon microscope equipped with excitation and barrier filters (470–510 nm) and a mercury lamp light source.

Electrophysiology—Gigaseals were formed using Sylgard-coated thin walled borosilicate pipettes (Kimax). Single channel currents were recorded with an Axopatch 200B patch clamp amplifier (Axon Instruments), digitized with a digital data recorder (VR10, Instrutech), and stored on video tape using a video tape recorder. The recorded signal was filtered at 3 kHz using an 8-pole Bessel filter (−3 dB, Frequency Devices) and transferred to a computer (Dell) using the Digidata 1200 interface (Axon Instruments) at a sampling rate of 10 kHz. The filter dead time was ~100 μs (0.3 F_c), and therefore events shorter than ~50 μs will be missed in our analysis. Single channel currents were ana-

lyzed using a pCLAMP program to obtain duration histogram, amplitude histogram, and channel activity (NP_o). N is the number of channels in the patch, and P_o is the probability of a channel being open. NP_o was determined from ~1–2 min of current recording. Macroscopic currents from COS-7 cells were recorded using the whole-cell or large outside-out configuration. Current tracings shown in figures were filtered at 1 kHz. Data are shown as mean ± S.D. Student's t test was used to test for significance between two values at the level of 0.05. For single channel studies at high $[K^+]_o$, the pipette and bath solutions contained 140 mM KCl, 2 mM $MgCl_2$, 10 mM HEPES, and 5 mM EGTA (pH 7.2). When studying the effect of pH and protein kinases, macroscopic currents were recorded using a physiological bath solution containing 118 mM NaCl, 1.3 mM KH_2PO_4, 25 mM $NaHCO_3$, 1.8 mM $CaCl_2$, 10 mM HEPES, 10 mM glucose, 4.7 mM KCl, and 1 mM $MgSO_4$. All experiments were performed at 23–25 °C.

RESULTS

Cloning of TASK-3—We used a 560-bp DNA fragment that encompasses the pore and C-terminal region of rat TASK-1 and screened rat cardiac and cerebellum cDNA libraries. One positive clone containing a partial sequence (1.7 kb) of a novel two-domain K^+ channel was obtained from screening the cerebellum cDNA library. After several rounds of screening using the 3′-region of the 1.7-kb DNA fragment as a probe, one positive clone containing the entire open reading frame of 1185 bases encoding a 395-amino acid polypeptide with a calculated molecular mass of 44 kDa was finally isolated (Fig. 1*A*). This clone had only a partial 3′-noncoding region and did not include the poly(A) sequence. Hydrophobicity analysis (25) of the amino acid sequence showed that the new clone belongs to the K^+ channel family with two pore-forming domains and four transmembrane segments (Fig. 1*B*). We placed the N terminus in the intracellular side, similar to those of other tandem pore K^+ channels. Thus, the putative K^+ channel subunit has a short N terminus, an extended extracellular loop between M1 and P1, and a long C terminus, structural features typical of nearly all 4TM K^+ channels (Fig. 1*C*). One *N*-glycosylation site is present in the extended extracellular loop between M1 and P1, similar to that found in several other K^+ channels of this class, including TASK-1 and TASK-2. The amino acid sequence of the new clone shows several potential phosphorylation sites. Consensus sites for protein kinase A are found in the intracellular loop between M2 and M3 (Thr-134), at the proximal site in the C terminus (Thr-247), and at the end of the C terminus (Ser-394). Three sites for protein kinase C are found all in the C terminus (Ser-277, Ser-340, Ser-352). Potential phosphorylation sites for tyrosine kinase were not present.

Searching the GenBank™ data base using the BLAST sequence alignment program (26) indicated that the DNA sequence of the new clone is most similar to that of TASK-1, a 4TM K^+ channel that was cloned earlier (20, 23, 27). A 2P/4TM K^+ channel clone named TASK-2 has been described recently but has low homology with that of TASK-1 or the new clone (21). We therefore named our new clone TASK-3. A putative homologue of rat TASK-3 was identified in the genome data base of human chromosome 8 (GenBank ™ accession number AC007869; locus D8S1741). Combined partial sequences from two locations with an intervening sequence of ~84 kb showed 72% identity in the amino acid sequence with rat TASK-3. Within the first 250 amino acids of rat TASK-3 and the human homologue, the identity was 94%. Fig. 2*A* shows alignment of three TASK sequences, which reveal high homology between TASK-1 and TASK-3, especially within the transmembrane and pore-forming domains. TASK-1 and TASK-3 share 54% identity and 61% similarity in amino acid sequences, whereas TASK-2 is distantly related with 27% amino acid identity with TASK-1 and 26% with TASK-3. Therefore, TASK-1 and TASK-3 probably share close functional similarity, although this has yet to be demonstrated. The dendrogram of all tandem pore K^+ channels identified in the mammalian system is shown in Fig. 2. The percentage indicates amino acid identity.

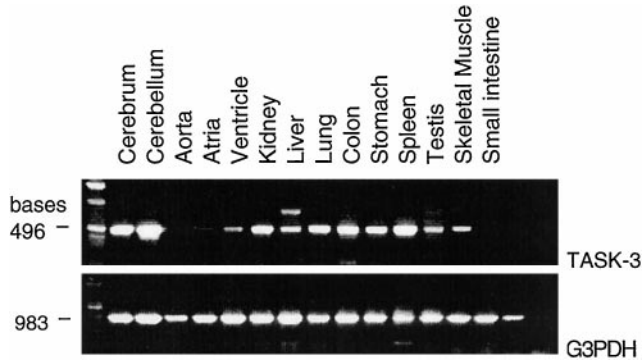

FIG. 3. **Reverse-transcriptase PCR analysis of TASK-3 in rat tissues.** Approximately 10 μg of total RNA from each tissue was used to prepare first strand cDNAs. TASK-3-specific primers were used to generate an expected PCR product of 496 bp. The amplified PCR products were subcloned into pCR2.1 vector (Invitrogen) and sequenced on one strand to verify the TASK-3 expression. Two controls (*last two lanes*) included one with the template DNA for glyceraldehyde-3-phosphate dehydrogenase (*G3PDH*) and one that has no cDNA (*last lane*). The quality of cDNA was checked using glyceraldehyde-3-phosphate dehydrogenase-specific primers (CLONTECH).

Tissue Distribution of TASK-3 mRNA—To determine which tissues express TASK-3 mRNA, Northern blot analysis was performed using rat multiple tissue blots (OriGene Technologies). No TASK-3 transcripts could be detected in the 12 tissues (Brain, heart, kidney, stomach, small intestine, muscle, spleen, thymus, liver, lung, testis, and skin), suggesting that TASK-3 mRNA is expressed at low levels or not expressed at all. To be sure of this result, we repeated the same experiment three times with new blots. In all three cases, no TASK-3 transcripts were detected. Under similar conditions and blots, we could clearly detect expression of TASK-1, as reported previously (23, 27). We therefore used RT-PCR to further examine the tissue distribution of TASK-3. Of the 14 tissues examined, the 496-bp PCR product of TASK-3 could be detected in most tissues. The relative signal was low in ventricle and barely detectable in the aorta, atria, and small intestine (Fig. 3).

Basic Electrophysiological Properties of TASK-3—To determine whether TASK-3 is capable of forming a functional ion channel, cDNA was subcloned into a mammalian expression vector (pcDNA3.1) and transfected along with DNA that encodes GFP into COS-7 cells. Whole cell currents were first recorded in solution containing 140 mM KCl (pipette and bath). Cell membrane potential was held at 0 mV and stepped to various potentials for a 500-ms duration. In cells transfected with GFP alone, only very small currents of less than 50 pA were recorded. In cells transfected with TASK-3/GFP, the same voltage steps produced large instantaneous and noninactivating currents (Fig. 4*A*). The whole-cell current varied nearly linearly with voltage as shown by the current-voltage relationship. A large fraction of the inward currents was reversibly blocked by 3 mM Ba^{2+} applied extracellularly. These results show that TASK-3 forms functional ion channels in COS-7 cells.

To characterize single channel properties of TASK-3, cell-attached patches were first formed. Nearly all COS-7 cells transfected with TASK-3 exhibited robust channel activity that did not decrease with time. Inside-out patches showed similar channel activity, indicating that TASK-3 is not regulated by soluble intracellular molecules in the cell under basal conditions. COS-7 cells transfected with GFP alone showed no such channel activity. Channel openings at different membrane potentials are shown in Fig. 4*B* when both pipette and bath

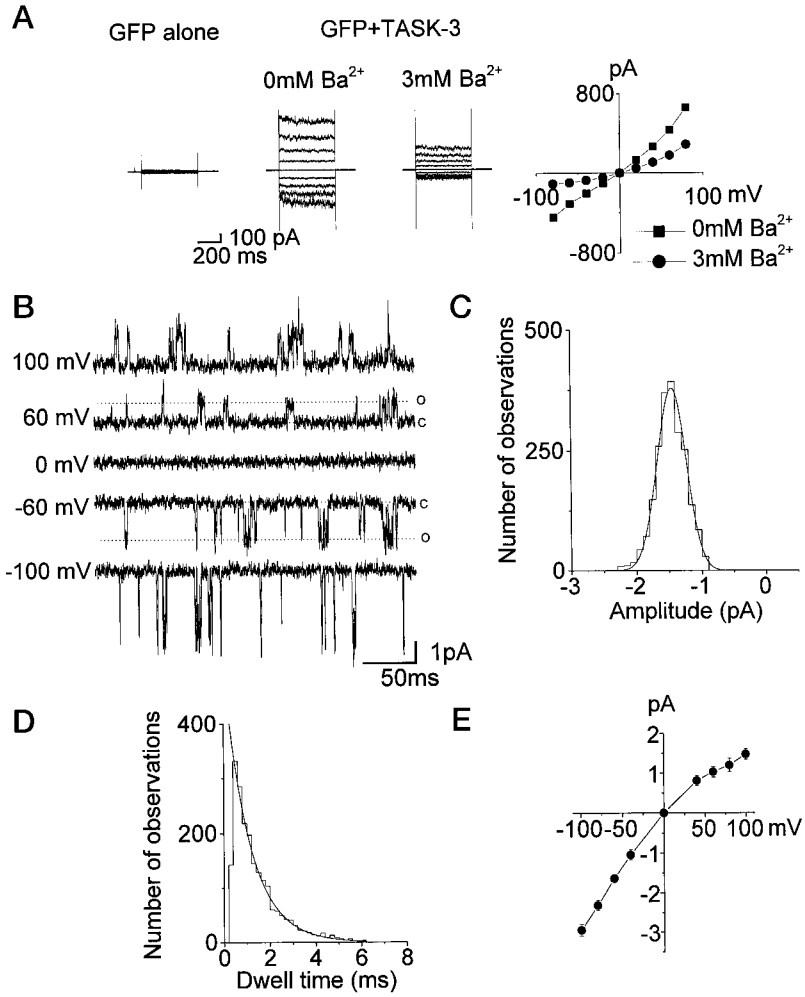

FIG. 4. **Expression of TASK-3 in COS-7 cells.** *A,* TASK-3 whole-cell currents were recorded from COS-7 cells transfected with DNA encoding TASK-3 and GFP. Pipette and bath solutions contained 140 mM KCl. The holding potential was 0 mV, and voltage steps were from −80 to +80 mV in 20 mV increments. The addition of 3 mM Ba^{2+} to the bath solution reversibly reduced TASK-3 current, as also shown in the current-voltage relationship. *B,* inside-out patches show inward and outward single channel openings at various membrane potentials in symmetrical 140 mM KCl. *C,* amplitude histogram of channel openings at −60 mV shows a single peak. *D,* duration histogram of openings at −60 mV in an inside-out patch containing only one channel is shown. The mean open time was 1.1 ms. *E,* current-voltage relationship of TASK-3 shows a weak inward rectification.

solutions contained 140 mM KCl. An amplitude histogram obtained from channel openings at −60 mV shows a single peak (Fig. 4*C*). The duration histogram obtained from a patch with only one level of channel opening shows that TASK-3 has a mean open time of 1.1 ± 0.1 ms at −60 mV (Fig. 4*D*; $n = 5$). The single channel current-voltage relationship shows that TASK-3 is a weak inward rectifier K^+ channel (Fig. 4*E*) similar to that observed with TASK-1 (23, 24). The conductances of TASK-3 were 27.1 ± 1.6 pS at −60 mV and 17.0 ± 2.2 pS at +60 mV.

Ion selectivity of TASK-3 was studied by changing the concentration of K^+ in the bath solution from 10 to 280 mM while maintaining the pipette $[K^+]$ constant at 140 mM. As shown in Fig. 5*A*, the reversal potential shifted to the right as $[K^+]$ in the bath solution was elevated, as expected of an ion channel that is permeable to K^+ but not to Cl^-. The plot of the reversal potential as a function of $[K^+]$ showed that the slope was 51 ± 3 mV/10-fold change in $[K^+]$, close to the calculated Nernst value of 58 mV (Fig. 5*B*). These results confirm that TASK-3 is a relatively K^+-selective ion channel, similar to TASK-1 and other two pore K^+ channels.

Pharmacological Studies—The effects of various pharmacological agents were examined on the TASK-3 current using outside-out patches from COS-7 cells. TASK-3 was insensitive to low concentrations of Ba^{2+} (<100 μM) and was blocked only at high concentrations (>300 μM). Ba^{2+} at 3 mM applied extracellularly blocked the inward TASK-3 current by 56 ± 9% ($n = 4$). TASK-3 was insensitive to 1 mM tetraethylammonium, 100 μM zinc chloride, and 170 mM ethanol. Quinidine (100 μM), lidocaine (1 mM), and bupivacaine (100 μM) caused 37 ± 6%, 62 ± 9%, and 56 ± 13%, respectively, inhibition of TASK-3 current ($n = 3$). Intracellular application of 10 μM Ca^{2+}, 30 mM Na^+, and 4 mM MgATP using inside-out patches had no significant effect on TASK-3 current ($n = 3$). However, GTPγS applied intracellularly produced a 30 ± 3% ($n = 4$) decrease in TASK-3 current, suggesting that a GTP-binding protein-dependent pathway regulates TASK-3 activity. Arachidonic acid (10 μM) showed a strong inhibitory activity from the intracellular side of the membrane, reducing TASK-3 current by 59 ± 4% ($n = 3$). TASK-3 channel activity in cell-attached or inside-out patches was insensitive to suction pressure applied to the patches (0 to −60 mm Hg).

TASK-3 possesses potential phosphorylation sites for both protein kinase A and C. Extracellular application of phorbol myristate acetate (100 nM), an activator of protein kinase C, failed to alter TASK-3 whole-cell current ($n = 5$). Application of 8-bromo-cyclic AMP (300 μM) and 1-methyl-3-isobutylxanthine (100 μM) together, which should increase cAMP concentration in the cell and activate protein kinase A, also failed to alter TASK-3 current. Forskolin (10 μM), an activator of adenylyl cyclase and 1-methyl-3-isobutylxanthine (100 μM) together, also did not affect TASK-3 current. Therefore, TASK-3 does not appear to be regulated via phosphorylation by protein kinases A and C.

Regulation of TASK-3 Current by pH—A hallmark of TASK-1 and TASK-2 K^+ channels is their sensitivity to pH_o. To determine whether TASK-3 also possesses similar pH sensitivity, we first examined TASK-3 current using large outside-out patches from COS-7 cells transfected with TASK-3 and GFP. Cell membrane potential was held at −80 mV and then a voltage ramp (−100 to +100 mV; 640 ms duration) was applied.

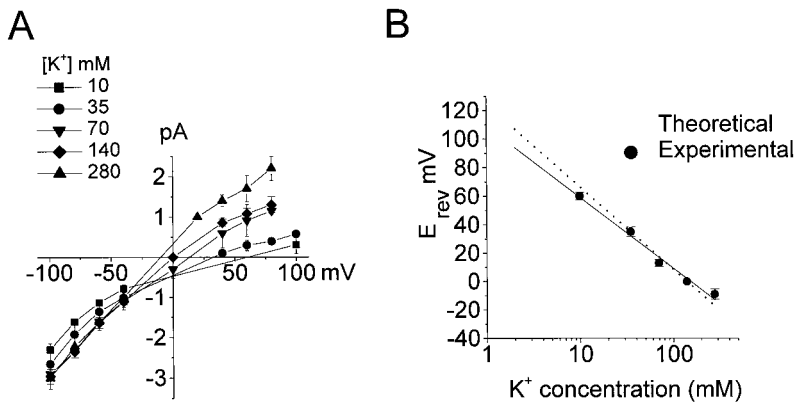

FIG. 5. **$[K^+]$-Dependence of the reversal potential.** *A,* inside-out patches were used to determine changes in reversal potential after changing $[K^+]$ in the bath solution. Current-voltage relationships were plotted at different $[K^+]_i$. Lines were drawn by eye. *B,* reversal potentials from three patches were determined and plotted as a function of $[K^+]$. The *dotted line* shows the slope from the Nernst equation (slope, 58 mV/decade). Experimental values were fitted by linear regression (slope, 51 mV/decade).

TASK-3 currents were measured at different pH_o values (Fig. 6*A*). TASK-3 was markedly inhibited by extracellular acidification (pH 6.0–7.2) at all membrane potentials. At pH_o 6.4 and 6.0, the current decreased to 74 ± 17% and 96 ± 3%, respectively, of that observed at pH_o 7.2. An increase in pH_o above 7.2 caused a small rise in TASK-3 current, showing that TASK-3 is less sensitive to changes in pH_o in the alkaline range (7.2–8.4). Averaged currents at different pH_o values at −20, +20, and +60 mV were determined from three experiments and plotted in Fig. 6*B*. The data were fitted to a Hill equation of the form: $y = 1/(1 + (k_{1/2}/[H^+])^n)$, where $k_{1/2}$ is the $[H^+]$ at which half maximal inhibition occurs and n is the Hill coefficient. At −20 mV, apparent $k_{1/2}$ was 1.8×10^{-7} M corresponding to a p*K* of 6.7, and the Hill coefficient was 2.0 (mean values, $n = 3$). At +20 mV, the p*K* and Hill coefficient were 6.7 and 1.8, respectively. For currents recorded at +60 mV, the p*K* and the Hill coefficient were 6.6 and 1.7, respectively.

To study in more detail the effect of changes in pH_o and pH_i on TASK-3 kinetics, we recorded single channel currents from outside-out and inside-out patches, respectively, at different pH_o values. Fig. 6*C* shows channel openings from an outside-out patch showing the effect of changing the pH_o of the bath solution from 7.2 to 6.4, 6.0, 8.0 and then back to 7.2. Amplitude histograms obtained from such tracings at different pH_o values are also shown. Current-voltage relationships show that the single channel conductance is not significantly altered between pH_o 6.0 and 7.2 (Fig. 6*D*). However, changing pH_o from 7.2 to 8.0 caused a significant increase in single channel conductance. Relative channel current was obtained by multiplying NP_o and single channel current (i) at −60 mV and then plotted as a function of pH_o. Fig. 6*E* shows that TASK-3 is particularly sensitive to changes in pH_o ranging from 6.0 and 7.2. These results show that the marked decrease in channel activity observed at low pH_o is predominantly because of a decreased frequency of opening. Fig. 6*F* shows results obtained from inside-out patches in which the pH of the bath solution (pH_i) was sequentially changed from 8.0 to 7.2, 6.4, and 6.0. Changing pH_i did not significantly affect the single channel conductance. At pH 6.4 and 6.0, TASK-3 current was 81 ± 9% and 77 ± 11%, respectively, of that observed at pH 7.2. These results show that TASK-3 is much more sensitive to pH_o than to pH_i and that the effect of pH_o is not mediated via changes in pH_i.

Histidine at Position 98 Confers pH_o Sensitivity—To identify the amino acid residue responsible for the marked sensitivity to pH_o, we mutated two histidine residues (His-72 and His-98) that are conserved in TASK-1 and TASK-3 (see Fig. 1). Four mutant TASK-3 (H72D, H72Q, H98D, and H72Q/H98D) were generated and tested for their pH_o sensitivity. Outside-out patches from COS-7 cells were used to measure single channel activity at different pH_o. The single channel conductance at pH 7.2 was 26 ± 2 pS for the H98D mutant and 33 ± 2 pS for the H72D mutant ($n = 4$), indicating that modifications of the long extracellular loop between TM1 and TM2 alter channel conductance. As shown in Fig. 7*A*, pH_o sensitivity of the H72D mutation was similar to that of wild type TASK-3. pH_o sensitivity of the H72Q mutant was also similar to that of the wild type TASK3, showing greater than 90% reduction in current by a decrease in pH_o from 7.2 to 6.0. However, the H98D or H72Q/H98D mutation abolished the acid-induced decrease in K^+ current (Fig. 7*B*). Therefore, the single histidine residue at position 98 is critical for the acid sensing of TASK-3.

DISCUSSION

A New Member of the "TASK" Family of K^+ Channels—We successfully isolated a new member of the K^+ channel family that possesses two pore-forming domains and four transmembrane segments. We named the new clone TASK-3 as it belonged to the acid-sensing TASK family of K^+ channels. TASK-3 is the 9th 4TM K^+ channel to be identified in the mammalian system (hence *KCNK9*), after TWIK-1 (13), TREK-1 (16), TASK-1 (20, 23), TRAAK (17), TASK-2 (21), TWIK-2 (28), *KCNK6,* and *KCNK7* (22). An insect 4TM K^+ channel named ORK1 (open rectifier K^+ channel 1) has been cloned earlier from *D. melanogaster* (12). TASK-3 is most closely related to TASK-1 both in nucleotide and amino acid sequences and functional channel behavior. Our study shows that expression of TASK-3 mRNA is very low in the rat heart, indicating that TASK-3 is unlikely to be a functional partner of TASK-1 whose mRNA is highly expressed in the rat heart. Therefore, TASK-3 probably serves as a functionally separate K^+ channel to regulate cell K^+ conductance in the cells that express it.

Electrophysiological Behavior of TASK-3—Single-channel conductances of TASK-1 and TASK-3 expressed in COS-7 cells are 14 and 27 pS, respectively, under identical ionic conditions (symmetrical 140 mM KCl (24)). With the exception of the third transmembrane segment, which has 64% amino acid identity with that of TASK-1, the pore and transmembrane sequences of TASK-3 are nearly identical to those of TASK-1. The kinetic behavior of TASK-3 is similar to that of TASK-1 in that they both open in short bursts with several closings within each burst. TASK-2 shows a much higher single channel conductance (60 pS) under similar ionic conditions and thus can be distinguished from TASK-1 and TASK-3 (21). These differences in single channel properties should help to subsequently identify the native K^+ channel with similar characteristics.

Like TASK-1 and other putative background K^+ channels, TASK-3 is open at all membrane potentials and its activity is simply a function of how far the membrane potential is set from the reversal potential. As TASK-3 is expressed in the brain, it may be involved in setting the resting membrane potential as

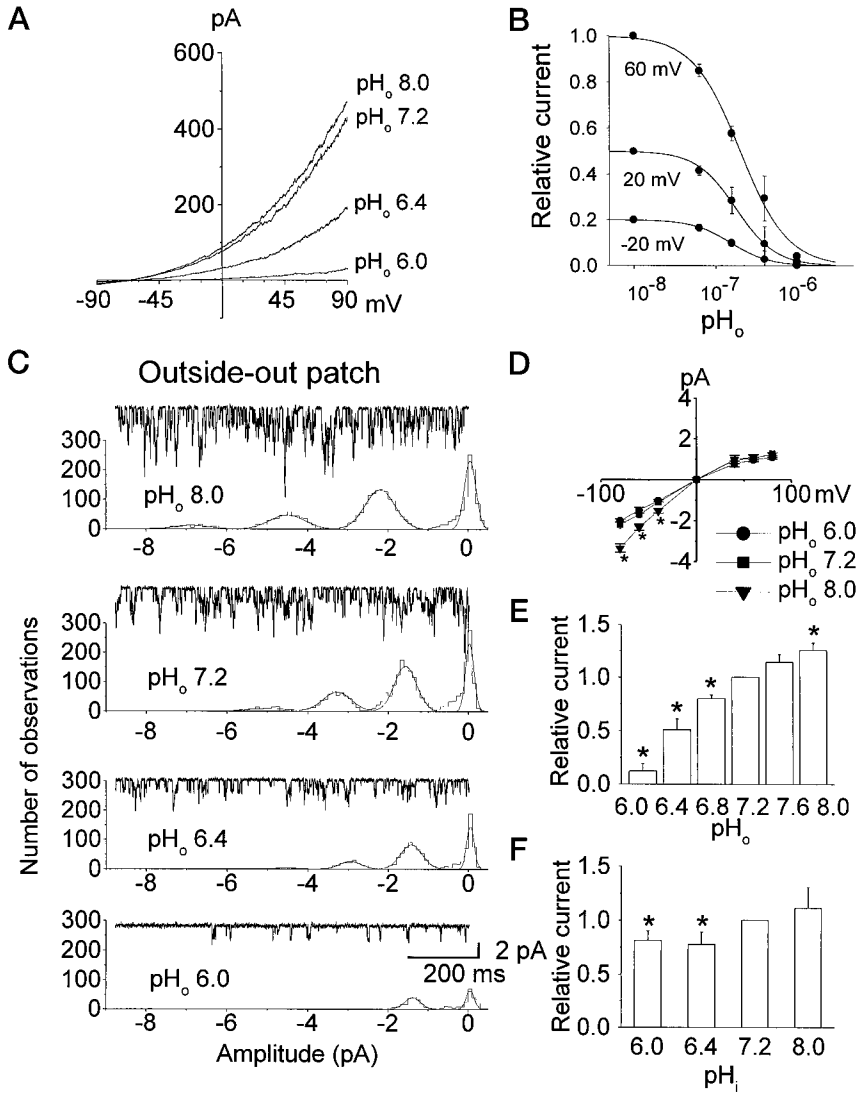

FIG. 6. **pH-dependent changes in TASK-3 current in COS-7 cells.** *A,* macroscopic currents were recorded from large outside-out patches containing many channels. Ramp protocol (−100 mV to +100 mV) was used to generate the current-voltage relations at different extracellular pH. *B,* relative currents at −20, +20, and +60 mV were determined and plotted as a function of extracellular pH. The points were fitted to a Hill equation and apparent pK ($k_{1/2}$) and Hill coefficients were determined (see "Results "). Each point is the mean ± S.D. of three determinations. *C,* single channel openings from one outside-out patch at different external pH are shown with amplitude histograms. *D,* current-voltage relationships obtained at different pH$_o$ are shown. *E,* bar graph shows relative channel current at different pH$_o$. The current at pH$_o$ 7.2 was taken as 1.0 (NP_o = 0.22 ± 0.05; n = 4). *F,* bar graph shows relative channel currents at different pH$_i$. The current at pH$_i$ 7.2 was taken as 1.0. Each bar is the mean ± S.D. of four determinations. The *asterisk* indicates a significant difference from the value at pH 7.2, as judged by paired t test.

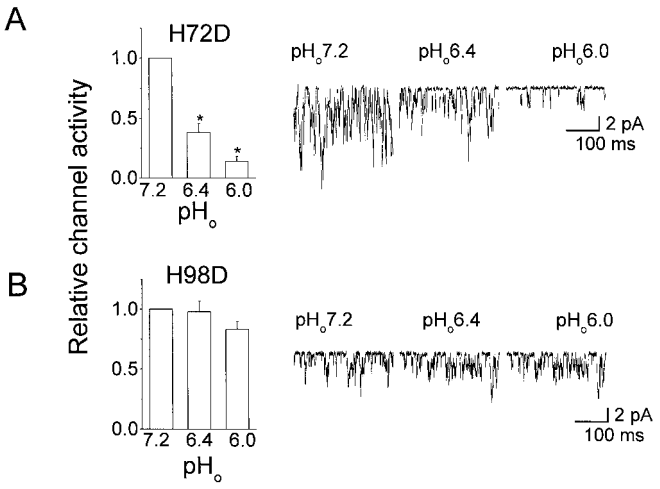

FIG. 7. **Histidine at position 98 confers pH$_o$ sensitivity.** Outside-out patches were formed from COS-7 cells transfected with a TASK3 mutant, H72D (*A*) or H98D (*B*). The effect of changes in pH$_o$ was tested as in Fig. 6, and relative channel activities are shown. Each bar is the mean ± S.D. of four determinations. The *asterisk* indicates a significant difference from the value at pH 7.2.

well as the action potential duration in certain neurons. Different types of background K^+ channels with lack of intrinsic voltage dependence have been reported in various type of cells (29–33). Therefore, one of the important tasks in the future will be to determine which tandem pore K^+ channel encodes the various native background K^+ channels in specific tissues.

Pharmacological Studies—TASK-3 was generally insensitive to K^+ channel blockers such as tetraethylammonium and Ba^{2+}, similar to the low sensitivity exhibited by TASK-1 and TASK-2 (20, 21, 27). TASK-3 is inhibited 40–60% by 100 μM quinidine, 1 mM lidocaine, and 100 μM bupivacaine, similar to TASK-1. However, TASK-3 is little affected by ethanol (170 mM) or zinc (100 μM), which blocks TASK-1 current by 40% (27) Interestingly, TASK-1 has been shown to be activated by inhalation anesthetics such as halothane and isoflurane (34), although the latter has been reported to have no effect in another study (27). We have not tested the effect of these agents on TASK-3 in this study. Inhalation anesthetics have been shown to activate TREK-1 (34), another tandem pore K^+ channel that is also activated by arachidonic acid and membrane tension. TASK-3 does not possess the PDZ binding motif (T/SXV) that is present in the carboxyl end of TASK-1 (23, 27). Although TASK-3 possesses putative phosphorylation sites for protein kinase A and C, we were unable to detect any effect of activators of these kinases in COS-7 cells. Thus, all three TASK K^+ channels appear to be generally insensitive to regulation by protein kinase A and C.

pH Sensitivity of TASK Family of K^+ Channels—The modulation by pH is an interesting and important functional prop-

erty of the TASK class of K^+ channels. Like TASK-1, TASK-3 exhibited greater sensitivity to changes in extracellular than intracellular pH. Our single channel studies using outside-out patches clearly identify the mechanism of the pH_o effect on TASK-3 as that produced mainly via changes in the number of channel openings in the pH_o 6.0–7.2 range. Our studies also show that the histidine residue located next to the GYG sequence, which is considered to be the selectivity filter of the channel, confers this pH_o sensitivity. At present, it is difficult to know the physiological roles of TASK-3. One could suspect that changes in pH_o that are known to occur under physiological and pathophysiological conditions would be expected to modulate cell function if cells display TASK currents. For example, in the brain, H^+ is known to mediate the changes in blood CO_2 and modulate the function of the cells in the brainstem that regulates respiration. pH shifts also occur during stimulus in various types of neurons (35–37). H^+ have been shown to cause pain by activating and modulating capsaicin receptors in certain neurons (38). If these neurons also show TASK currents, changes in H^+ because of inflammation may also modulate pain generation. In pathological conditions such as ischemia and seizure, altered metabolism would clearly lead to lowering of the extracellular pH (37). Although the role of TASK in these processes remains to be studied, the discovery of TASKs with high pH sensitivity strengthens the view that pH is an important modulator of physiological function in certain cell types.

REFERENCES

1. Rudy, B. (1988) *Neuroscience* **25,** 729–749
2. Jan, L. Y., and Jan, Y. N. (1994) *Nature* **371,** 119–122
3. Pongs, O. (1992) *Physiol. Rev.* **72,** 569–588
4. Ketchum, K. A., Joiner, W. J., Sellers, A. J., Kaczmarek, L. K., and Goldstein, S. A. N. (1995) *Nature* **376,** 690–695
5. Lesage, F., Guillemare, E., Fink, M., Durprat, F., Lazdunski, M., Romey, G., and Barhanin, J. (1996) *J. Biol. Chem.* **271,** 4183–4187
6. Reid, J. D., Lukas, W., Shafaatian, R., Bertl, A., Scheurmann-Kettner, C., Guy, H. R., and North, R. A. (1996) *Recept. Channels* **4,** 51–62
7. Isacoff, E. Y., Jan, Y. N., and Jan, L. Y. (1990) *Nature* **345,** 530–534
8. Heginbotham, L., Lu, Z., Abramson, T., and Mackinnon, R. (1994) *Biophys. J.* **66,** 1061–1067
9. Doyle, D. A., Morais, J., Pfuetzner, R. A., Kuo, A., Gulbis, J. M., Cohen, S. L., Chait, B. T., and Mackinnon, R. (1998) *Science* **280,** 69–77
10. Wei, A., Jegla, T., and Salkoff, L. (1996) *Neuropharmacology* **35,** 805–829
11. Wang, Z. W., Kunkel, M. T., Wei, A., Butler, A., and Salkoff, L. (1999) *Annu. N. Y. Acad. Sci.* **868,** 286–303
12. Goldstein, S. N., Price, L. A., Rosenthal, D. N., and Pausch, M. H. (1996) *Proc. Natl. Acad. Sci. U. S. A.* **93,** 13256–13261
13. Lesage, F., Guillemare, E., Fink, M., Duprat, F., Lazdunski, M., Romey, G., and Barhanin, J. (1996) *EMBO J.* **15,** 1004–1011
14. Goldstein, S. A. N., Wang, K.-W., Ilan, N., and Pausch, M. H. (1998) *J. Mol. Med.* **76,** 13–20
15. Pountney, D. J., Gulkarov, I., Vega-Saenz de Miera, E., Holmes, D., Saganich, M., Rudy, B., Artman, M., and Coetzee, W. A. (1999) *FEBS Lett.* **450,** 191–196
16. Fink, M., Duprat, F., Lesage, F., Reyes, R., Romey, G., Heurteaux, C., and Lazdunski, M. (1996) *EMBO J.* **15,** 6854–6862
17. Fink, M., Lesage, F., Duprat, F., Heurteaux, C., Reyes, R., Fosset, M., and Lazdunski, M. (1998) *EMBO J.* **17,** 3297–3308
18. Patel, A. J., Honore, E., Maingret, F., Lesage, F., Fink, M., Duprat, F., and Lazdunski, M. (1998) *EMBO J.* **17,** 4283–4290
19. Maingret, F., Fosset, M., Lesage, F., Lazdunski, M., and Honore, E. (1999) *J. Biol. Chem.* **274,** 1381–1387
20. Duprat, M., Lesage, F., Fink, M., Reyes, R., Heurteaux, C., and Lazdunski, M. (1997) *EMBO J.* **16,** 5464–5471
21. Reyes, R., Duprat, F., Lesage, F., Fink, M., Salinas, M., Farman, N., and Lazdunski, M. (1998) *J. Biol. Chem.* **273,** 30863–30869
22. Salinas, M., Reyes, R., Lesage, F., Fosset, M., Heurteaux, C., Romey, G., and Lazdunski, M. (1999) *J. Biol. Chem.* **274,** 11751–11760
23. Kim, D., Fujita, A., Horio, Y., and Kurachi, Y. (1998) *Circ. Res.* **82,** 513–518
24. Kim, Y., Bang, H. W., and Kim, D. (1999) *Am. J. Physiol.* **277,** H1669–H1678
25. Kyte, J., and Doolittle, R. (1982) *J. Mol. Biol.* **157,** 162–166
26. Altschul, S. F., Gish, W., Miller, W., Myers, E. W., and Lipman, D. J. (1990) *J. Mol. Biol.* **215,** 403–410
27. Leonoudakis, D., Gray, A. T., Winegar, B. D., Kindler, C. H., Harada, M., Taylor, D. M., Chavez, R. A., Forsayeth, J. R., and Yost, C. S. (1998) *J. Neurosci.* **18,** 868–877
28. Chavez, R. A., Gray, A. T., Zhao, B. B., Kindler, C. H., Mazurek, M. J., Mehta, Y., Forsayeth, J. R., and Yost, C. S. (1999) *J. Biol. Chem.* **274,** 7887–7892
29. Baker, M., Bostock, H., Grafe, P., and Martius, P. (1987) *J. Physiol.* (*Lond.*) **383,** 45–67
30. Koh, D. S., Jonas, P., Brau, M. E., and Vogel, W. (1992) *J. Membr. Biol.* **130,** 149–162
31. Shen, K. Z., North, R. A., and Surprenant, A. (1992) *J. Physiol.* (*Lond.*) **445,** 581–599
32. Koyano, K., Tanaka, K., and Kuba, K. (1992) *J. Physiol.* (*Lond.*) **454,** 231–246
33. O'Kelly, I., Stephens, R. H., Peers, C., and Kemp, P. J. (1999) *Am. J. Physiol.* **276,** L96–L104
34. Patel, A. J., Honore, E., Lesage, F., Fink, M., Romey, G., and Lazdunski, M. (1999) *Nature Neurosci.* **2,** 422–426
35. Chesler, M. (1990) *Prog. Neurobiol.* (*N. Y.*) **34,** 401–427
36. Krishtal, O. A., Osipchuk, Y. V., Shelest, T. N., and Smirnoff, S. V. (1987) *Brain Res.* **436,** 352–356
37. Siesjo, B. K., von Hanwehr, R., Nergelius, G., Nevander, G., and Ingvar, M. (1985) *J. Cereb. Blood Flow Metab.* **5,** 47–57
38. Caterina, M. J., Schumacher, M. A., Tominaga, M., Rosen, T. A., Levine, J. D., and Julius, D. (1997) *Nature* **389,** 816–824

TASK-3, a New Member of the Tandem Pore K^+ Channel Family

Yangmi Kim, Hyoweon Bang and Donghee Kim

J. Biol. Chem. 2000, 275:9340-9347.
doi: 10.1074/jbc.275.13.9340